Apr 29th, 8:00 AM

Paper Session II-B - Early Results from the Space Telescope Imaging Spectograph

B. Woodgate
NASA/Goddard Space Flight Center, Space Telescope Imaging Spectograph Instrument Definition Team

R. Kimble
NASA/Goddard Space Flight Center, Space Telescope Imaging Spectograph Instrument Definition Team

C. Bowers
NASA/Goddard Space Flight Center, Space Telescope Imaging Spectograph Instrument Definition Team

S. Kraemer
NASA/Goddard Space Flight Center, Space Telescope Imaging Spectograph Instrument Definition Team

M. E. Kaiser
NASA/Goddard Space Flight Center, Space Telescope Imaging Spectograph Instrument Definition Team

See next page for additional authors

Presenter Information

B. Woodgate, R. Kimble, C. Bowers, S. Kraemer, M. E. Kaiser, A. Danks, J. Grady, J. Loaicono, D. Hood, W. Meyer, C. VanHouten, V. Arabright, R. Bybee, J. G. Timothy, M. Blouke, D. Dorn, M. Bottema, R. Woodruff, D. Michika, J. Sullivan, J. Hetlinger, R. Stocker, M. Brumfield, L. Feinberg, A. Delamere, D. Rose, H. Garner, D. Linder, T. Gull, S. Heap, C. Joseph, R. Green, E. Jenkins, J. Linsky, J. Hutchings, H. W. Moos, A. Boggess, S. Maran, F. Roesler, D. Weistrop, G. Sonneborn, G. Bower, and J. Gardner

Early results from the Space Telescope Imaging Spectrograph.

B. Woodgate [ab], R. Kimble [ab], C. Bowers [ab], S. Kraemer [ab], M. E. Kaiser [ab], A. Danks [ab], J. Grady [a], J. Loiacono [a], D. Hood [c], W. Meyer [c], C. VanHouten [c], V. Argabright [c], R. Bybee [c], J. G. Timothy [b], M. Blouke [d], D. Dorn [c], M. Bottema [c], R. Woodruff [c], D. Michika [c], J. Sullivan [c], J. Hetlinger [c], R. Stocker [c], M. Brumfield [a], L. Feinberg [a], A. Delamere [c], D. Rose [c], H. Garner [c], D. Lindler [a], T. Gull [ab], S. Heap [ab], C. Joseph [b], R. Green [be], E. Jenkins [b], J. Linsky [b], J. Hutchings [b], H. W. Moos [b], A. Boggess [b], S. Maran [ab], F. Roesler [b], D. Weistrop [b], G. Sonneborn [a], G. Bower [e] and J. Gardner [a].

[a] NASA/Goddard Space Flight Center, Greenbelt, MD 20771

[b] Space Telescope Imaging Spectrograph Instrument Definition Team (STIS/IDT)

[c] Ball Aerospace and Technologies Corporation, Boulder , CO 80303

[d] SITe Corporation, Beaverton, OR 97077

[e] NOAO, Tucson, AZ 85726

Abstract

The STIS instrument was installed into HST in February 1997 during the Servicing Mission 2. It has completed checkout and is beginning its science program, and is working well. Several scientific demonstration observations were taken, illustrating some of the range of scientific uses and modes of observation of STIS.

Keywords: Hubble, spectrograph, echelle, ultraviolet, optical, spectra, MAMA, black hole, galaxies, supernova

1. Introduction

STIS was built by Ball Aerospace for the Laboratory for Astronomy and Solar Physics at NASA/Goddard Space Flight Center. It is a UV and visible spectrograph with a wavelength range from 115 to 1000 nm, and has spectral resolving powers between 20 and 100,000. It uses 2-dimensional detectors with 1024 x 1024 pixels, a CCD in the visible/IR and Multi-Anode Microchannel Arrays (MAMAs) in the UV. The 2 MAMAs, one with CsI and one with CsTe, were built at Ball. Use of 2-dimensional detectors allows direct imaging, long slit spectroscopy to obtain many spectra of an extended object at once, and echelle spectroscopy for simultaneous high spectral resolution and broad spectral range. The primary spectral modes are shown in the Table.

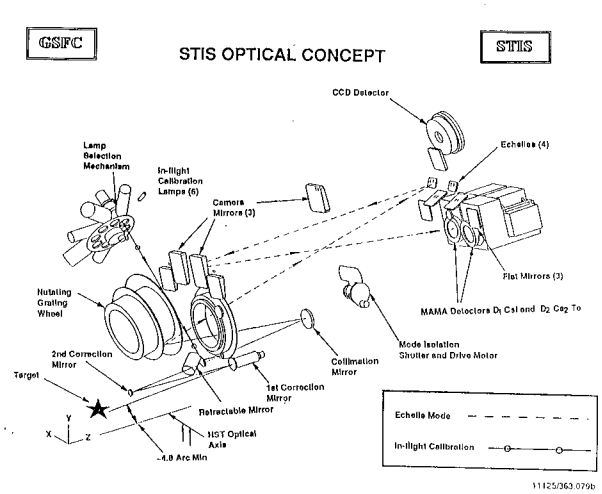

***Figure 1**. STIS optical layout.*

The optical layout is shown in Figure 1. Light entering the instrument is first corrected for spherical aberration and astigmatism to produce a sharp image at the entrance slit wheel of the spectrograph, where one of 65 small slits, long slits or large apertures can be selected. The spectrograph collimator then puts a parallel beam onto the grating wheel, where one of 21 gratings, mirrors or a prism is selected, defining the spectral mode. The grating wheel also tilts to direct the beam to a detector or mirror or echelle grating, and selects the wavelength range[1,2,3].

Table. Primary STIS science modes

Mode	Band Wavelength range (nm) Detector	Band 1 (FUV) 115-170 MAMA/CsI	Band 2 (NUV) 165-310 MAMA/Cs_2Te	Band 3 (VIS) 305-555 CCD	Band 4 (NIR) 550-1000 CCD
Low resolution spectral imaging	Mode name Spectral resolving power Specified throughput Exposures/band	G140L 770-1130 3.8% 1	G230L 415-730 3.0% 1	G430L 445-770 13.0% 1	G750L 425-680 14.2% 1
Medium resolution spectral imaging	Mode name Spectral resolving power Specified throughput Exposures/band	G140M 8600-12800 2.2% 11	G230M 7500-13900 2.0% 18	G430M 4340-7730 12.0% 10	G750M 3760-6220 13.2% 10
Medium resolution echelle	Mode name Spectral resolving power Specified throughput Exposures/band	E140M 50,000 0.93% 1	E230M 35,000 1.0% 2	N/A	N/A
High resolution echelle	Mode name Spectral resolving power Specified throughput Exposures/band	E140H 150,000 0.64% 3	E230H 140,000 0.69% 6	N/A	N/A
Very low resolution spectroscopy	Mode name Spectral resolving power Specified throughput	N/A	PRISM 165-26 3.3%	N/A	N/A
Camera	Mode name	FUV	NUV	CCD	CCD/LP

2. Early Observations

During the post-launch checkout phase prior to the start of the primary science program, a few early observations were taken to demonstrate the new scientific capability and show some of the ways in which STIS will operate.

2.1. Supernova 1987A

For the special case of extended emission line objects we can observe with wide slit spectroscopy to obtain many separate images at once of an object. For example for SN 1987A, a supernova that exploded in the Large Magellanic Cloud (LMC), a small galaxy close to our own 160,000 light years away, we selected an area including the inner fossil ring and part of the outer rings surrounding the supernova, using our 2 x 52 arcsec slit, as shown between the blue lines in the upper left of Figure 2.[4] Selected spectral images show lines of [NII], H alpha and [NII] in the upper right, two [SII] lines in the center, and [OIII] at the bottom right. The images of the inner ring are slightly different sizes in the different lines This 1.2 light year diameter ring was ejected by the star in its earlier red giant stage about 20,000 years ago, and was recently heated and ionized by the UV flash of the supernova explosion. We now see the 50,000K afterglow of this event, and can derive the properties of the ring by the structure and decay of the different line images.

In the brighter [NII] image, we see the fainter outer ring to the right broken at the location of the central supernova. We interpret this as shadowing of the ring by the extended supernova blast wave, showing that the left side of the right outer ring is behind the supernova. This tells us the orientation of the entire three ring system, that the left ring is in front and the right ring is behind.

In several of the images we see a gap in the ring, at about 2 o'clock. In the hydrogen and oxygen line images there is an emission feature interior to this point, which we interpret as blue-shifted line emission from the gap. Since we know now that this ring edge is towards us, blue-shifted emission is moving away from the supernova. This suggests that the first parts of the blast wave front are beginning to impact and break through the ring. The velocity measured is 250 km/s (? M mph).

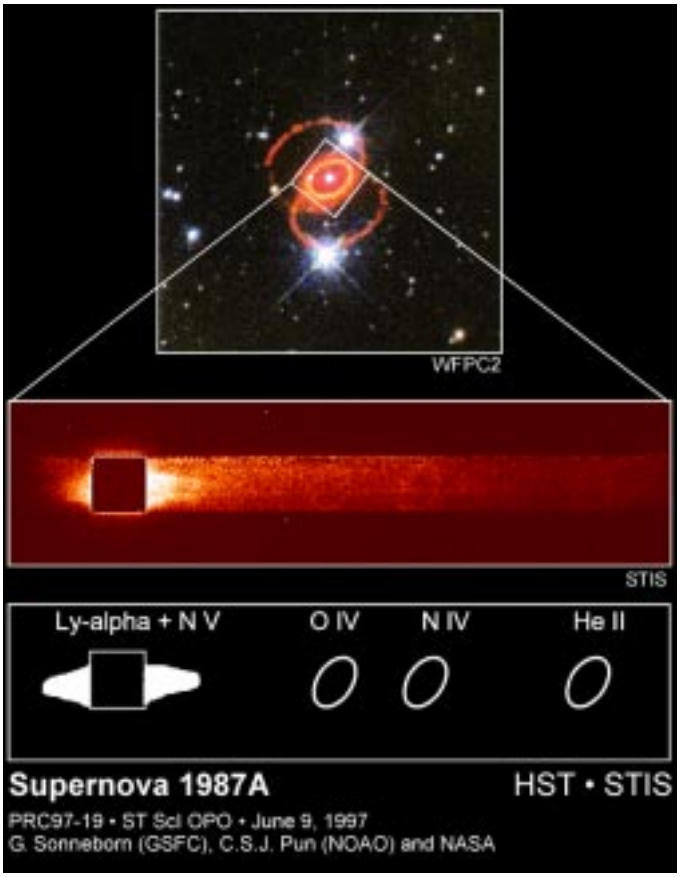

Figure 2. Supernova 1987A in the visible.

Top left: WFPC image with STIS 2 arcsec wide slit superposed.

Top right: Spectral images of emission lines of [NII], H alpha and [NII]. The outer ring seen in the right [NII] image is shadowed by the central supernova debris, showing the left sides of the rings are behind the right sides. Blue-shifted emission from the gap in the inner ring at 2 o'clock shows material blasting out through the ring.

Center: Spectral emission lines of [SII]. Ratio shows the density in the ring is greater than 10^3 cm^{-3}.

Center right: Spectral emission line of [OIII]. Shows blue-shifted component.

We then obtained a UV spectrum through a 2 x 2 arcsec slit, to include the inner ring and to exclude a nearby bright star (Figure 3). The Lyman alpha bright earth airglow is shown blocked out. Three faint rings in the lines of [OIV], [NIV] and HeII are just detectable. High velocity H Lyman alpha and NV emission is seen surrounding the supernova, but interior to the ring, with a velocity about 15,000 km/s (33 M mph). This emission was predicted from X-ray and radio observations to be from the blast wave of the supernova debris hitting the surrounding low density gas, and we are now able to see its location. We expect it to get much brighter when the main blast hits the ring in a few years.

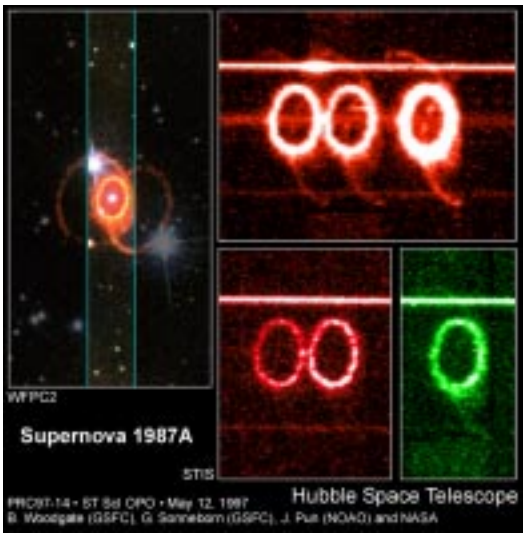

Figure 3. *Supernova 1987A in the UV. Top: WFPC image with STIS 2 x 2 arcsec aperture superposed. Center: STIS UV spectral image. Bright H Lyman alpha geocorona has been blocked out. Lyman alpha and NV emission from high velocity gas (15,000km/s) from the supernova blast wave interacts with the circumstellar gas. Bottom: Cartoon identifying features.*

2.2. A black hole in a galaxy center

Figure 4 shows the result of observations of slit spectroscopy of the galaxy M84 in the Virgo cluster of galaxies 50 million light years away.[5] The left image is a WFPC picture of the center of the galaxy with the position of the STIS slit superposed. Spectra as a function of position along the slit were recorded in the emission lines of H alpha, [NII] and [SII], and a strong wavelength shift was seen across the nucleus, 400 km/s within 26 light years, as shown on the right. Only a black hole has mass sufficiently concentrated to produce such a large shift in such a small distance. As the gas is sucked in to the black hole, it orbits around it, glowing from the energy it gains from the gravitational field. The mass of the black hole is greater than one billion suns, and may be larger depending on the tilt angle of the axis of rotation to us.

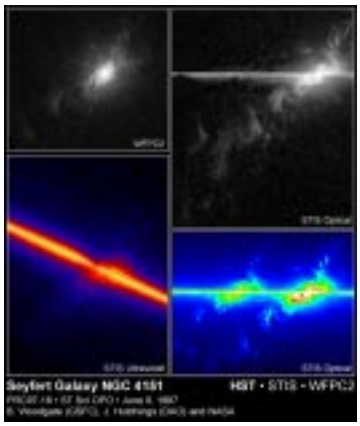

Figure 4. *Black hole in the center of the Virgo cluster galaxy M84. Left: WFPC image with STIS 0.2 arcsec wide slit superposed. Right: Plot of center wavelength of emission lines along the slit shows a black hole mass at least one billion suns.*

2.3. Funnel clouds from a galaxy nucleus

If a black hole at the center of a galaxy is fed rapidly with gas and stars it exhibits a variety of violent behaviors, and is called an active galactic nucleus (AGN). Spiral galaxies with AGNs are called Seyfert galaxies.

If an emission line object is sufficiently isolated and free of continuum light, spectra may be taken with a large aperture, and the separate images in the emission lines recorded. In Figure 5 the upper left shows an image taken by WFPC in the [OIII] filter of the nearby Seyfert galaxy NGC 4151. Many knots are seen to the lower left and upper right of the nucleus. STIS spectra were taken in the G430M mode, and the lower right image shows the spectral image with two [OIII] lines.[6] The weaker image to the left was subtracted, leaving the image shown on the upper right. Comparing this with the WFPC filter image in the same line, we see the inner knots are streaked out in the spectral direction in STIS. Below the nuclear continuum line spectrum, the knots are streaked out to the left or short wavelength side, and above the line are shifted to longer wavelengths. By comparing the positions of each knot we find its velocity towards or away from us. This reveals a pattern of knots flowing out in a double cone, with the material in the lower cone flowing towards us and in the upper cone away from us, at up to 1000 km/s.

Further out the more distant knots do not share in this outflow. The velocities are reversed, possibly from general motions of the galaxy or a backflow into the central cone.

Figure 5. *Bipolar outflows from the Seyfert nucleus in NGC 4151. Top left: WFPC [OIII]5007 image. Top right: STIS [OIII]5007 spectral image, showing knots smeared by doppler shift near the nucleus. Bottom right: [OIII]5959 and 5007 spectral image. Bottom left: UV spectral image showing doppler shifted CIV emission close to the nucleus.*

2.4. Absorption spectra of supernova shells

UV spectra of a star show absorption features due to the intervening interstellar medium. STIS spectra of a star behind the Vela supernova remnant were taken in the FUV high resolution echelle mode E140H, which has an approximate resolving power R=150,000 (2 km/s).[7] We used a time-tag mode of data collection where each event's position and time (x,y,t) are telemetered down. The doppler shift contribution due to the orbital motion of 14 km/s was removed on the ground. The resulting spectrum is shown in Figure 6, showing that 50 echelle orders were recorded in one exposure. Several blocks of complex absorption line structure are seen. Each block is due to the absorption in a different spectral line from the complex velocity structure of the expanding filamentary shells formed by the shock waves from the supernova explosion impacting interstellar clouds. The velocity range is 210 km/s.

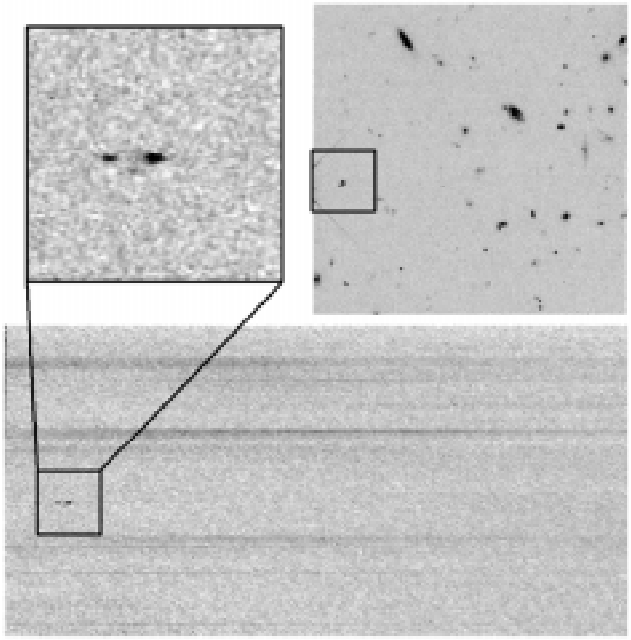

Figure 6*. Echelle spectrum of a star behind the Vela supernova remnant. Broad absorption line blocks are each spectral lines broken up by the velocity structure of the high velocity shocks from the supernova shells interacting with the interstellar medium.*

2.5. Parallel spectra of high redshift galaxies

Much of the early data taken by STIS will be in parallel with prime operations of the WFPC and NICMOS instruments. While we cannot select the field of view, we can take spectra of many objects at once by using the 50 x 50 arcsec aperture in the low resolution grating modes, combined with a direct image to provide a wavelength reference. We are currently using the G750L mode, primarily to capture compact emission line galaxies which should show up as near point-like sources in the spectra, at a variety of redshifts in the emission lines of [OII]3727, [OIII]5007, H alpha and Lyman alpha. Figure 7 shows an image and spectrum of a galaxy at redshift 0.804, emitting in the [OIII]5007 and 4959 lines redshifted to above 9000A.[8] The upper right panel is a direct image, the lower panel is a spectrum of the same region with the [OIII] lines standing out clearly, and the upper left is a close-up of those emission lines.

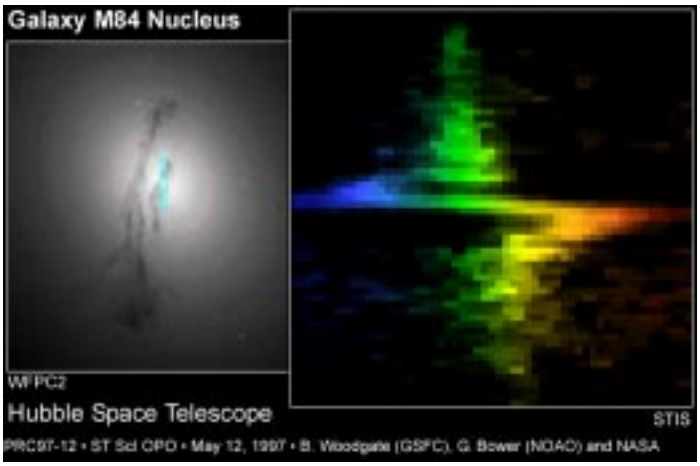

Figure 7. *Emission line galaxy at redshift 0.8 in STIS parallel data.*

Top right: CCD clear image, 2100 sec exposure, 50 x 50 arcsec field. Note compact objects just above the center near the left edge.

Bottom: Wide field spectrum of the same area as the image, 8400 sec exposure. Most galaxies show continuum spectra. The compact objects noted show emission lines of [OIII]4959 and 5007, and possibly of H beta, yielding a redshift of 0.804.

2.6 Planetary aurorae.

The UV detectors in STIS are insensitive to the visible, and so can select out the faint far UV emission from the aurorae of planets from the much brighter reflected light from the Sun in the visible. The improved UV sensitivity and higher spatial resolution of STIS enables planetary aurorae to be seen without rotational blurring and with more detail than before, and enables variations with time to be followed.

Figure 8 shows STIS far UV images of Jupiter's polar regions superposed on a WFPC visible image of the disk [9]. The high latitude rings are aurorae from particles originally generated from volcanoes on Jupiter's satellite Io falling in down Jupiter's magnetic field lines. The slightly lower latitude streaks are due to particles directly from Io, which is magnetically connected to the surface of Jupiter at these latitudes. The emission in each case is from the Lyman alpha line of hydrogen. The structures rotate with Jupiter, since the magnetic axis is offset from the rotational axis.

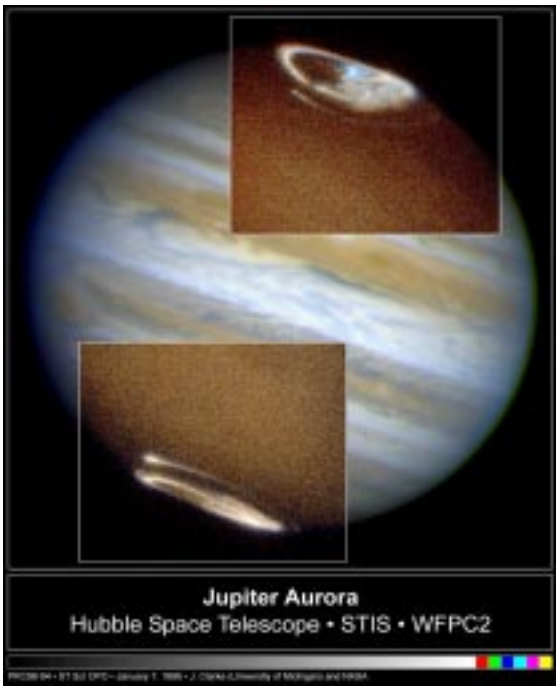

Figure 6*. Echelle spectrum of a star behind the Vela supernova remnant.*

Broad absorption line blocks are each spectral lines broken up by the velocity structure of the high velocity shocks from the supernova shells interacting with the interstellar medium.

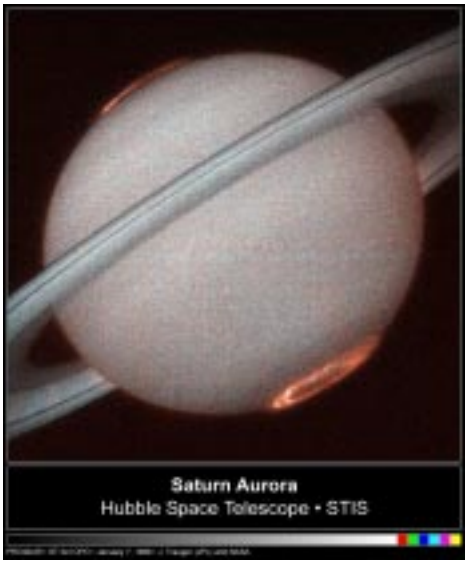

Figure 9. *Aurorae on Saturn.*

The auroral rings formed above the surface of Saturn, shown in this far UV image, are due to molecular hydrogen , selected by a cut-off filter to remove the atomic hydrogen Lyman alpha.

Figure 9 shows the auroral rings formed above the surface of Saturn in this far UV image. The rings shown here are due to molecular hydrogen , selected by a cut-off filter to remove the atomic hydrogen Lyman alpha[10]. This time-tagged image has been subdivided in time to reveal flickering structures in the aurorae. A similar image in the light of atomic hydrogen shows more extensive structure.

2.7. Protoplanetary disks.

Planetary systems are thought to be formed from equatorial gas and dust disks, themselves formed as the forming star condenses from interstellar clouds. The best studied protoplanetary disk, that around the star Beta Pictoris, was observed by STIS using its coronagraphic mask , which removes most of the light from the star, allowing the much fainter reflected light from the disk to be seen (Figure 10). This allowed the disk to be seen closer to the star than in previous observations, into a distance equivalent to that of Neptune from the Sun. The warp may be due to planets forming within the disk, or due to a companion white dwarf or a passing star.

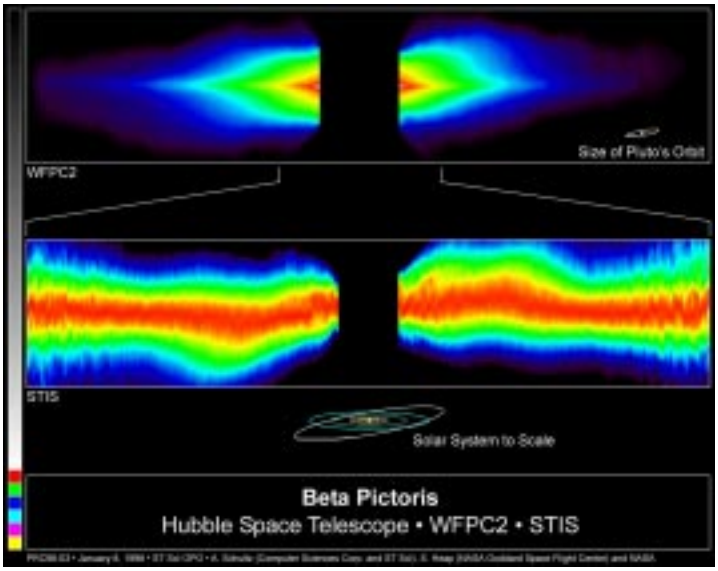

Figure 10. *The warped protoplanetary disk around Beta Pictoris.*

The warped disk, observed with the STIS coronagraphic mask, is seen closer to the star than in previous observations, equivalent to the distance of Neptune from the Sun. The warp may be due to planets forming within the disk, or due to a passing star.

Top: WFPC2 image, showing the outer parts of the disk.

Bottom: STIS image, showing the inner parts of the disk.

Acknowledgements

We thank the very large number of people that have contributed to STIS, at the Goddard Space Flight Center, the prime contractor Ball Aerospace, their subcontractors, and the STScI, over the 15 years since its inception.

References

1. B. E. Woodgate et al, “Capabilities of the Space Telescope Imaging Spectrograph (STIS) with smaller detectors”, in *Science with the Hubble Space Telescope*, P. Benvenuti and E. Shreier, eds., pp 525-534, 1992.
2. Woodgate, B. E. et al , “Design of the Space Telescope Imaging Spectrograph”, in preparation
3. Kimble, R. A. et al, “The on-orbit performance of the Space Telescope Imaging Spectrograph”, 1998, *Ap.J. Letters*, 492, L83.
4. Sonneborn, G. et al, “Spatially resolved STIS spectroscopy of SN 1987A: Evidence for shock interaction with circumstellar gas”, 1988, *Ap.J. Letters*, 492, L139.
5. Bower, G. et al, “Kinematics of the nuclear ionized gas in the radio galaxy M84 (NGC4374)”, 1988, *Ap.J. Letters*, 492, L111.
6. Hutchings, J. et al, “Gas cloud kinematics near the nucleus of NGC 4151”, 1988, *Ap.J. Letters*, 492, L115.
7. Jenkins, E. et al, “Ultraviolet absorption lines from high-velocity gas in the Vela supernova remnant: New insights from STIS echelle observations of HD72089”, 1988, *Ap.J. Letters*, 492, L147.
8. Gardner, J. et al, “The STIS parallel survey: Introduction and first results”, 1988, *Ap.J. Letters*, 492, L99.
9. Clarke, J., 1998, Press conference at January AGU:
http://oposite.stsci.edu/pubinfo/pr/1988/AAS_winter.html
10. Trauger, J. 1998, Press conference at January AAS:
http://oposite.stsci.edu/pubinfo/pr/1988/AAS_winter.html
11. Heap, S. 1998, Press conference at January AAS:
http://oposite.stsci.edu/pubinfo/pr/1988/AAS_winter.html